Electronic Supplementary Material (ESI) for Physical Chemistry Chemical Physics.

Supporting Information:

CASPT2 Study of Inverse Sandwich-Type Dinuclear 3d Transition Metal Complexes of Ethylene and Dinitrogen Molecules: Similarities and Differences in Geometry, Electronic Structure, and Spin Multiplicity

Masayuki Nakagaki and Shigeyoshi Sakaki*

Fukui Institute for Fundamental Chemistry, Kyoto University, Takano-Nishihiraki-cho, Sakyo-ku, Kyoto 606-8103, Japan

Corresponding author: E-mail: sakaki.shigeyoshi.47e@st.kyoto-u.ac.jp

Table S1 Relative energies (kcal/mol) of η^1-end and η^2-side structures calculated by CASPT2 method with two different active spaces.

	Co in quintet		Ni in triplet	
	(8e,8o)	(12e,10o)	(6e,6o)	(14e,10o)
$\Delta E(\eta^2\text{-}\eta^1)$				
CASSCF	5.2	4.6	14.9	13.3
CASPT2	4.8	5.3	2.5	15.1
Reference weight of CASSCF wavefunction				
η^1-end	0.683	0.690	0.676	0.678
η^2-side	0.685	0.688	0.664	0.679

In the dinitrogen ISTCs of Co and Ni, we carried out CASPT2 calculations with larger active space including π orbitals. In the ISTC of Co, the relative energy between side-on and end-on structures is different little between the smaller and larger active spaces; see Table S1. This result indicates that the π orbitals are not important in the Co complex and also in the Sc to Mn complexes which exist in the left-hand side of Co in the periodic table; remember that the π orbitals become more important as going from the left-hand side to the right-hand side in the periodic table because the d orbital becomes more stable in energy as going to the right-hand side from the left-hand side. In the ISTC of Ni, however, the relative stabilities of the end-on and side-on coordination structures are somewhat different between the smaller and larger active spaces. This is because d-orbital energy becomes lower as going from Co to Ni and the CT from the π orbital of dinitrogen to the metal becomes stronger in the Ni complex to contribute to the larger stability of the end-on structure. Judging from these results, we employed the active space without the π orbitals for M = Sc to Co but the active space including the π orbitals for M = Ni.

In the ethylene ISTC of Ni, however, the π orbital could not be included in the active space because the π orbital went out from the active space during CASSCF calculation. This result indicates that the π orbital is not important in the active space of the ethylene ISTCs. We did not include the π orbital in the active space of these ethylene complexes.

Table S2. Eigenvalues of (μ-η^2:η^2-N_2)[Cr(AIP)]$_2$ including spin orbit coupling calculated by an effective one-electron Fock-type spin–orbit Hamiltonian is used suggested by Hess and coworkers. The geometry of singlet spin state was taken.

Absolute energy / a.u.	Relative energy / cm^{-1}	J_eff	Omega
-2657.03326924	0.00	0.0	0.0
-2657.03304100	50.09	1.0	1.0
-2657.03304100	50.09	1.0	0.0
-2657.03304100	50.09	1.0	1.0
-2657.03259705	147.53	2.0	2.0
-2657.03259705	147.53	2.0	1.0
-2657.03259705	147.53	2.0	0.0
-2657.03259705	147.53	2.0	1.0
-2657.03259705	147.53	2.0	2.0
-2657.03196453	286.35	3.0	3.0
-2657.03196453	286.35	3.0	2.0
-2657.03196453	286.35	3.0	1.0
-2657.03196453	286.35	3.0	0.0
-2657.03196453	286.35	3.0	1.0
-2657.03196453	286.35	3.0	2.0
-2657.03196453	286.35	3.0	3.0
-2657.03119342	455.59	4.0	4.0
-2657.03119342	455.59	4.0	3.0
-2657.03119342	455.59	4.0	2.0
-2657.03119342	455.59	4.0	1.0
-2657.03119342	455.59	4.0	0.0
-2657.03119342	455.59	4.0	1.0
-2657.03119342	455.59	4.0	2.0
-2657.03119342	455.59	4.0	3.0
-2657.03119342	455.59	4.0	4.0

Table S3. Important geometrical parameters of D_{2h}-optimized structures of $(\mu\text{-}\eta^2\text{:}\eta^2\text{-}C_2H_4)[Cr(AIP)]_2$ at the singlet to nonet spin states.

spin multiplicity	r(Cr-C)	r(C-C)
9	2.233	1.544
7	2.231	1.542
5	2.230	1.540
3	2.229	1.539
1	2.228	1.538

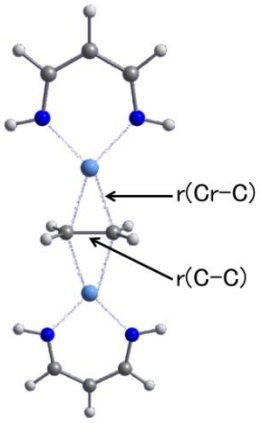

Table S4. Effective magnetic moment (μ_B) estimated by Boltzmann distribution law at 293 K with various geometries.

	CASSCF	CASPT2
D_{2h}-optimized	4.0	1.6
C_{2h}-optimized	4.9	2.0
X-ray(DDP)[a)]	3.7	1.5

a) The substituents were replaced by hydrogen atoms and position of all hydrogen atoms were optimized by DFT(B3LYP) method.

(A) Elongation of Cr-Cr distance

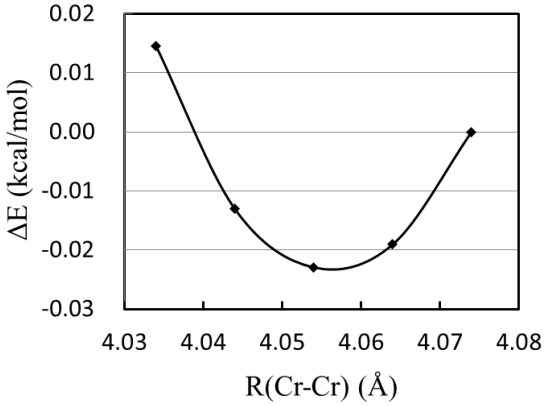

(B) Rotation of C_2H_4 moiety

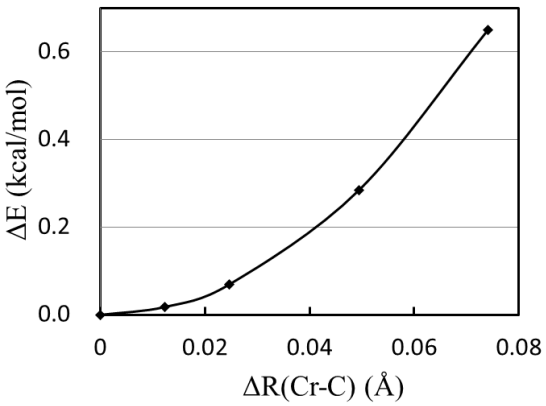

Figure S1. Potential energies of singlet spin state of (μ-C_2H_4)[Cr(AIP)]$_2$ at various (A) Cr-Cr distance and (B) orientation of ethylene calculated by the CASPT2 method. The CASSCF-optimized structures were used for other geometrical parameters.

Table S5. Similarities and differences between (μ-C_2H_4)[M(AIP)]$_2$ and (μ-N_2)[M(AIP)]$_2$ (M = Sc to Ni).

		Sc	Ti	V	Cr	Mn	Fe	Co	Ni
	Coordination geometry	Planer μ-η^2:η^2 (D_{2h})	Planer μ-η^2:η^2 (D_{2h})	Planer μ-η^2:η^2 (D_{2h})	Planer μ-η^2:η^2 (D_{2h})	Td-like μ-η^1:η^1 (C_{2h})	Td-like μ-η^1:η^1 (C_{2h})	Td-like μ-η^1:η^1 (C_{2h})	Td-like μ-η^1:η^1 (C_{2h})
C_2H_4	Spin state[a)]	OS	OS	OS	OS	OS	OS	OS	OS
	Energy difference[b)]	0.3	0.5	0.6	0.8	0.3	0.3	0.3	0.3
	Spin density on C_2H_4	~0	~0	~0	~0	~0	~0	~0	~0
	Coordination geometry	η^2-side	η^2-side	η^2-side	η^2-side	η^2-side ~η^1-end	η^1-end	η^1-end	η^1-end
N_2	Spin state[a)]	OS	OS	OS	OS	nonet	septet	quintet	triplet
	Energy difference[b)]	0.4	0.8	0.4	0.4	5.0	7.3	11.3	23.3
	Spin density on N_2	~0	~0	~0	~0	negative	negative	negative	negative

a) OS = open-shell singlet. b) Energy difference between the ground state and the next spin state.

(A) Lone pair orbital of AIP ligand

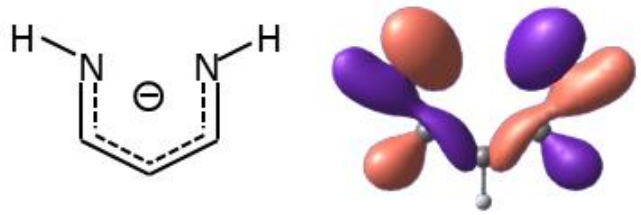

(B) MOs between AIP and M d orbitals

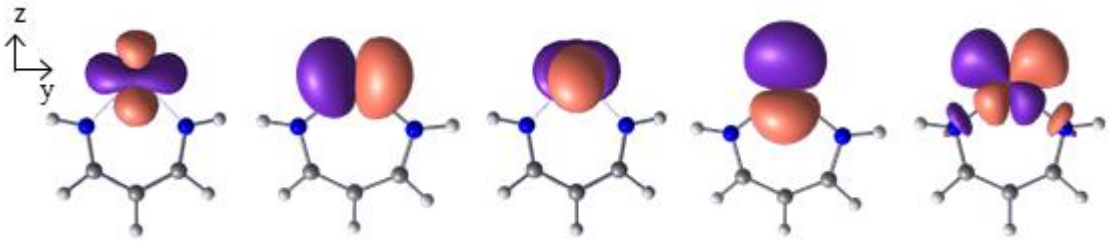

φ_1 φ_2 φ_3 φ_4 φ_5

(C) One example of bonding and anti-bonding pairs, φ_5^b and φ_5^a of $[M(AIP)]_2$

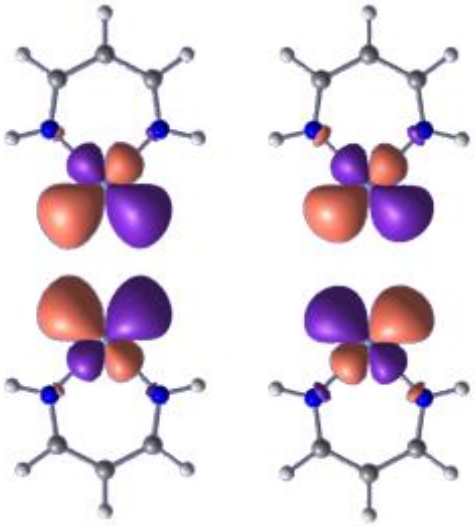

φ_5^b φ_5^a

Figure S2. MO diagram of M(AIP).

Anti-bonding and bonding pairs of d orbitals, φ_i^a and φ_i^b (i=1 to 5) are formed in the $[M(AIP)]_2$ moiety, which are nearly degenerate because of the long M-M distance. The φ_i^a and φ_i^b represent anti-bonding and bonding pairs of two d orbitals, respectively.

In an isolated M(AIP), the d_{yz} orbital is considerably destabilized in energy by the anti-bonding overlap with the two lone pair orbitals of the AIP ligand; see Figure S3(A) for the lone pair orbitals of AIP. Other four d orbitals are nearly degenerate at a lower energy than the d_{yz} because they are nearly non-bonding, as shown in Figure S3(B). Because two M(AIP) moieties are involved in one ISTC, anti-bonding and bonding pairs of d orbitals, φ_i^a and φ_i^b (i=1 to 5), are formed in the $[M(AIP)]_2$ moiety; see Figure S3 (C) for instance. These φ_i^a and φ_i^b MOs are nearly degenerate because of the long M-M distance. The φ_5^a, which is an anti-bonding pair of the d_{yz} orbitals of two Cr centers, overlaps well with the π^* orbital of ethylene to form the bonding $\psi_{1,b2g}$ MO and anti-bonding $\psi_{11,b2g}$ MO in $(\mu\text{-}\eta^2\text{:}\eta^2\text{-}C_2H_4)[Cr(AIP)]_2$. The φ_5^b is a bonding pair of the d_{yz} orbitals of two Cr centers, which is nearly non-bonding.

The reason why the benzene ISTC of Cr has a high spin ground state

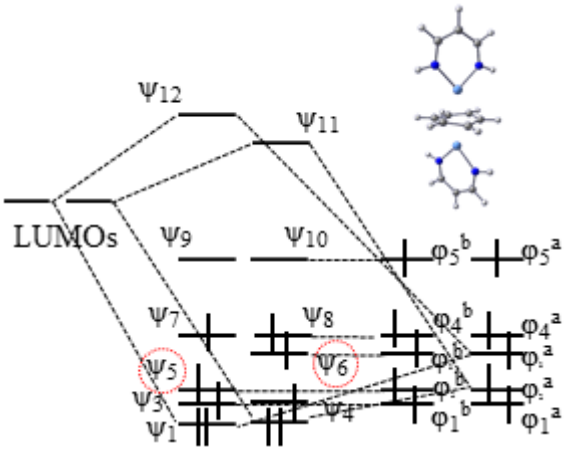

C_6H_6 (μ-C_2H_4)[Cr(AIP)]$_2$ [Cr(AIP)]$_2$

Figure S3. Schematic orbital interaction diagrams of (μ-η^6:η^6-C_6H_6)[Cr(AIP)]$_2$

In the benzene ISTC, the d_{x2-y2} and d_{xy} orbitals form bonding ψ_1 and ψ_2 MOs with the LUMO of benzene. The ψ_5 and ψ_6, which are non-bonding MOs consisting of d_{x2-y2} and d_{xy} orbitals, respectively, are singly occupied, as shown in Figure S2. The one-electron excitation from the ψ_1 and ψ_2 MOs to the ψ_9 and ψ_{10} MOs induces the exchange interaction with the singly occupied ψ_5 and ψ_6 MOs, which corresponds to the spin polarization. Because the high spin state can receive the energy stabilization by this spin-polarization, the benzene ISTC of Cr has a high spin ground state.

(A) d_{xz} orbital Cr(occ), V(vir), Ti(vir), Sc(vir)

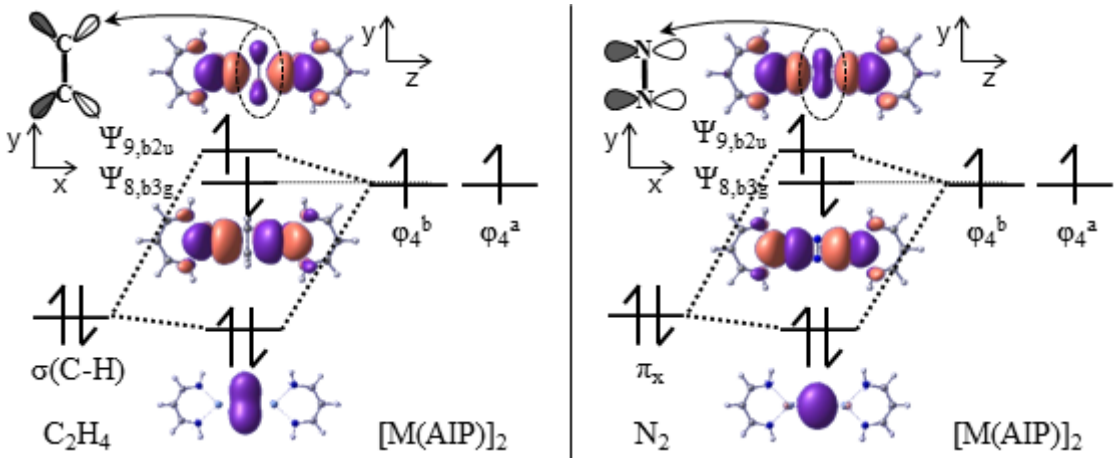

(B) d_{z2-y2} orbital Cr(occ), V(occ), Ti(vir), Sc(vir)

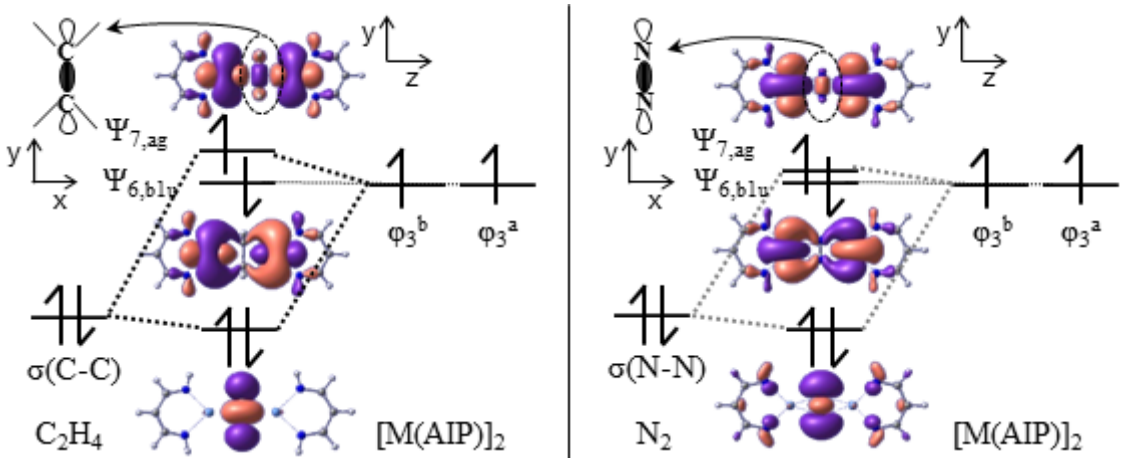

(C) d_{xy} orbital Cr(occ), V(occ), Ti(occ), Sc(vir)

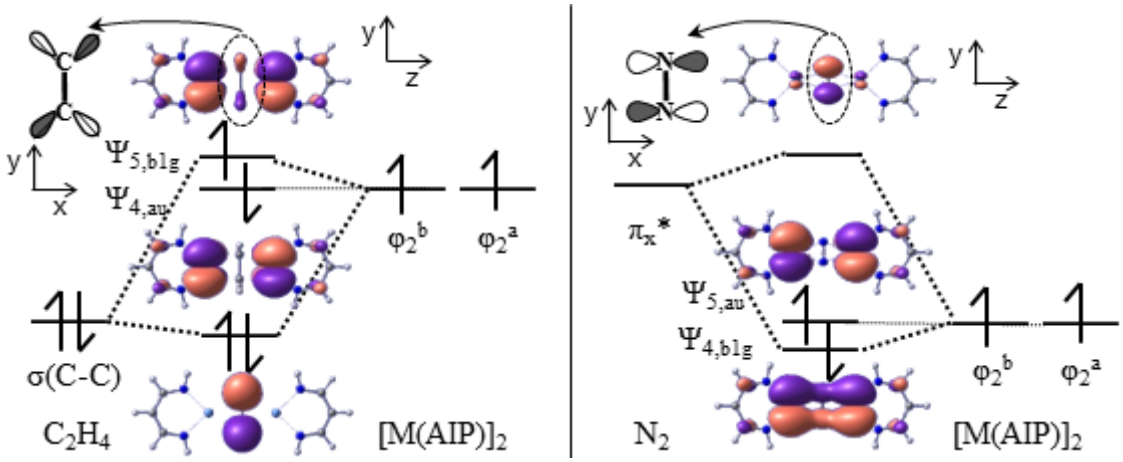

(D) d_{x2} orbital Cr(occ), V(occ), Ti(occ), Sc(occ)

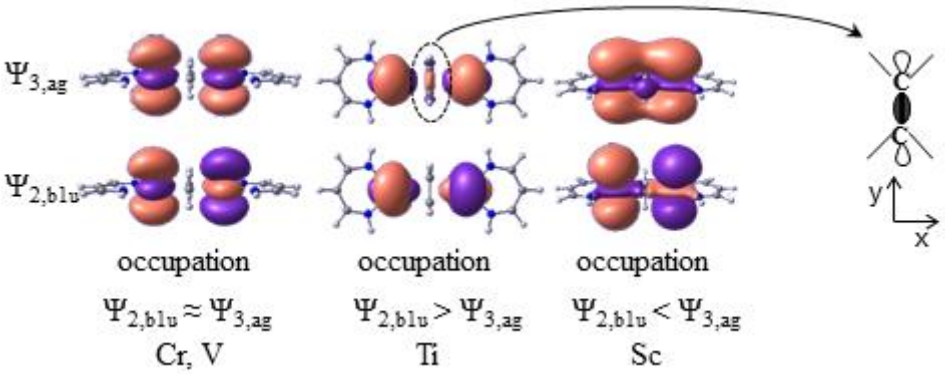

Figure S4. Schematic pictures of orbital energy splitting between bonding and anti-bonding pair d orbitals in $(\mu\text{-}\eta^2\text{:}\eta^2\text{-}C_2H_4)[M(AIP)]_2$ and $(\mu\text{-}\eta^2\text{:}\eta^2\text{-}N_2)[M(AIP)]_2$ (M = Sc to Cr).

The explanation of the occupation numbers in the $\psi_{2,b1u}$ and $\psi_{3,ag}$

In the Cr and V complexes, the $\psi_{2,b1u}$ and $\psi_{3,ag}$ mainly consist of the metal d_{x2} orbitals. Because the d orbital is compact, the $\psi_{2,b1u}$ and $\psi_{3,ag}$ are almost degenerate, leading to the presence of similar occupation numbers in these two orbitals; see Table 3.

In the Ti complex, the occupation number of the $\psi_{3,ag}$ is moderately larger than that of $\psi_{2,b1u}$. Because the size of d orbital is larger in Ti than in V, the anti-bonding overlap between the doubly occupied C-H σ-orbitals of ethylene and the φ_1^b increases in the $\psi_{3,ag}$, which leads to the smaller occupation number in the $\psi_{3,ag}$ than in $\psi_{2,b1u}$.

Because the size of d orbital becomes further larger in Sc than in Ti, a direct bonding overlap between two d_{x2} orbitals is formed in the $\psi_{2,b1u}$. Thus, the larger occupation of $\psi_{3,ag}$ than that of the $\psi_{2,b1u}$ is favorable to stabilize the system.

Table S6. Relative energies (in kcal/mol) of various spin multiplicities in (μ-C_2H_4)[M(AIP)]$_2$ (M = Cr, Mn) with D_{2h} and C_{2h} structures calculated by the CASSCF method.

spin multiplicity	Cr		Mn	
	C_{2h}	D_{2h}	C_{2h}	D_{2h}
11			0.00	31.5
9	1.1	6.0	0.02	31.0
7	0.8	5.4	0.04	30.6
5	0.4	4.8	0.05	30.3
3	0.1	4.4	0.06	30.1
1	0.0	4.2	0.06	30.0

(A) η^2-side-on (B) η^1-end-on

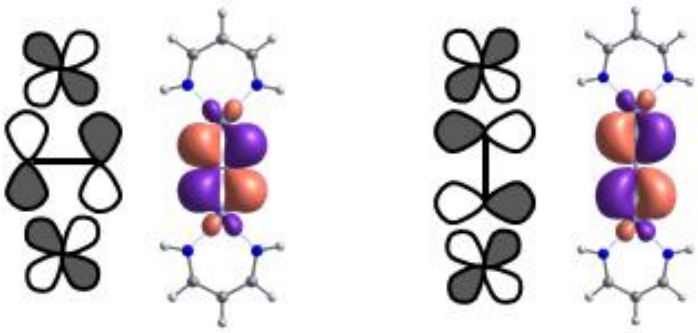

Figure S5. The bonding $\psi_{1,b2g}$ MO of (μ-N_2)[Cr(AIP)]$_2$ with (A) η^2-side-on and (B) η^1-end-on coordination structures. The $\psi_{1,b2g}$ MO in the η^1-end-on structure is less stable in energy than that of η^2-side-on one because of the smaller d_π-π^* overlap than in the η^2-side-on structure.

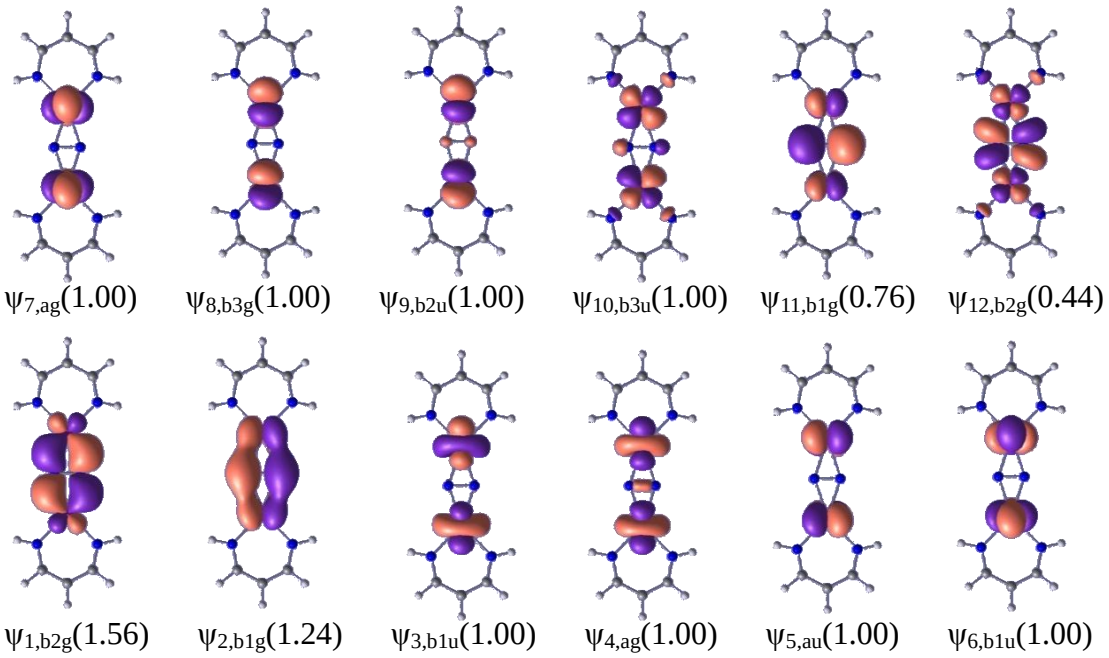

Figure S6. CASSCF-calculated natural orbitals of (μ-η^2:η^2-N_2)[Mn(AIP)]$_2$. The subscript represents irreducible representation under D_{2h} symmetry. In parentheses are occupation numbers in the nonet state.

Table S7. Orbital energies (in eV) of π and π^* orbitals of C_2H_4 and N_2 calculated by the HF method.

		cc-pVDZ	cc-pVTZ	cc-pVQZ	cc-pV5Z
C_2H_4	π^*	4.7	4.2	3.9	3.6
	π	−10.2	−10.2	−10.3	−10.3
N_2	π^*	4.8	4.4	4.2	3.9
	π	−16.5	−16.7	−16.7	−16.7

Table S8. Main electron configurations of the CASSCF wavefunction with natural orbitals and the CASCI wavefunction with localized orbitals of (μ-N_2)[Mn(AIP)]$_2$.

(A) ^9A_u state in η^1-end-on

CASSCF with natural orbitals

Configuration												Coefficient
ψ_1	ψ_2	ψ_3	ψ_4	ψ_5	ψ_6	ψ_7	ψ_8	ψ_9	ψ_{10}	ψ_{11}	ψ_{12}	
2	2	α	α	α	α	α	α	α	α	0	0	0.5630
2	α	α	α	α	α	α	α	α	α	ß	0	0.3378
α	2	α	α	α	α	α	α	α	α	0	ß	−0.2845
2	0	α	α	α	α	α	α	α	α	2	0	−0.2409
0	2	α	α	α	α	α	α	α	α	0	2	−0.2273
ß	2	α	α	α	α	α	α	α	α	0	α	0.2137
2	ß	α	α	α	α	α	α	α	α	α	0	−0.1927

CASCI with localized orbitals

Configuration												Coefficient
[M(AIP)]$_2$										N_2		
φ_1^a	φ_1^b	φ_2^a	φ_2^b	φ_3^a	φ_3^b	φ_4^a	φ_4^b	φ_5^a	φ_5^b	π^*_y	π^*_x	
α	α	α	α	α	α	α	α	α	α	ß	ß	0.8150
α	α	α	α	α	α	α	α	α	2	0	ß	0.2079
α	α	α	α	α	α	α	2	α	α	ß	0	−0.2014
α	α	α	α	α	α	α	α	α	ß	α	ß	−0.1659
α	α	α	α	α	α	α	α	α	0	2	ß	−0.1569
α	α	α	α	α	α	α	ß	α	α	ß	α	−0.1542

(B) $^{9}B_{2u}$ state in η^2-side-on

CASSCF with natural orbitals

Configuration												Coefficient
ψ_1	ψ_2	ψ_3	ψ_4	ψ_5	ψ_6	ψ_7	ψ_8	ψ_9	ψ_{10}	ψ_{11}	ψ_{12}	
2	α	α	α	α	α	α	α	α	α	ß	0	0.5290
2	2	α	α	α	α	α	α	α	α	0	0	−0.4778
2	0	α	α	α	α	α	α	α	α	2	0	0.2728
ß	α	α	α	α	α	α	α	α	α	ß	α	−0.2573
0	α	α	α	α	α	α	α	α	α	ß	2	−0.2044
α	α	α	α	α	α	α	α	α	α	ß	ß	0.1848
α	2	α	α	α	α	α	α	α	α	α	ß	−0.1820

CASCI with localized orbitals

Configuration												Coefficient
[M(AIP)]$_2$										N_2		
φ_1^a	φ_1^b	φ_2^a	φ_2^b	φ_3^a	φ_3^b	φ_4^a	φ_4^b	φ_5^a	φ_5^b	π^*_y	π^*_x	
α	α	α	α	α	α	α	α	α	α	ß	ß	0.8138
α	α	α	α	α	α	α	α	0	α	2	ß	0.2424
α	α	α	α	α	α	α	α	2	α	0	ß	0.2301
α	α	α	α	α	α	α	α	ß	α	α	ß	0.2111
α	α	α	α	α	α	α	α	α	ß	α	ß	0.1483
α	α	α	α	α	α	2	α	α	α	ß	0	−0.1143

Table S9. Occupation numbers of CASSCF natural orbitals in $[(\mu\text{-}\eta^2\text{:}\eta^2\text{-}C_2H_4)[Cr(AIP)]_2]^-$ and $[(\mu\text{-}\eta^2\text{:}\eta^2\text{-}C_2H_4)[Mn(AIP)]_2]^+$.

	$[(\mu\text{-}\eta^2\text{:}\eta^2\text{-}C_2H_4)[Cr(AIP)]_2]^-$	$[(\mu\text{-}\eta^2\text{:}\eta^2\text{-}C_2H_4)[Mn(AIP)]_2]^+$
$\psi_{11,b2g}$	0.19	0.47
$\psi_{10,b3u}$	1.00	1.00
$\psi_{9,b2u}$	1.00	1.00
$\psi_{8,b3g}$	1.00	1.00
$\psi_{7,ag}$	1.00	1.00
$\psi_{6,b1u}$	1.00	1.00
$\psi_{5,b1g}$	1.00	1.00
$\psi_{4,au}$	1.00	1.00
$\psi_{3,ag}$	1.00	1.00
$\psi_{2,b1u}$	1.00	1.00
$\psi_{1,b2g}$	1.81	1.53